DOI: 10.1002/ejic.201001202

Donor-Acceptor Couples and Late Transition Metal Complexes of Oxidation-Labile 1,4,5,8-Tetrakis(guanidino)naphthalene Superbases

Viktoriia Vitske,[a] Pascal Roquette,[a] Simone Leingang,[a] Christian Adam,[a] Elisabeth Kaifer,[a] Hubert Wadepohl,[a] and Hans-Jörg Himmel*[a]

Keywords: Nickel / Cobalt / Copper / Dinuclear complexes / Donor-acceptor systems / Redox chemistry / Magnetic properties / Superbases / Guanidines

In this manuscript the reactivity of the two oxidation-labile superbases 1,4,5,8-tetrakis(*N*,*N*,*N*′,*N*′-tetramethylguanidino)-naphthalene and the newly synthesized 1,4,5,8-tetrakis(*N*,*N*′-dimethyl-*N*,*N*′-ethylene-guanidino)naphthalene (tdmegn) are discussed and compared with that of related organic electron donors. The work includes oxidation with inorganic and organic oxidation reagents, as well as the preparation and characterization of dinuclear Co^{II}, Ni^{II} and Cu^{I} complexes. Magnetic coupling in the dinuclear Co^{II} and Ni^{II} complexes is studied on the basis of SQUID measurements. Finally, the results of experiments on the oxidation of the dinuclear Cu^{I} complexes are presented.

Introduction

In the past decades, a number of organic proton sponges and superbases were synthesized and applied for various purposes.[1] The classical proton sponge 1,8-bis(dimethylamino)naphthalene was described already in 1968 by Alder et al.[2] Due to resonance stabilization of the conjugated acid, guanidines are much stronger bases than amines. For example, the guanidines $HNC(NMe_2)_2$ and $MeNC(NMe_2)_2$ exhibit pK_a values of 23.3 and 25.0, respectively, in CH_3CN.[3] With the bisguanidine 1,8-bis(*N*,*N*,*N*′,*N*′-tetramethylguanidino)naphthalene (btmgn, see Scheme 1),[4] a combination of Alder's proton sponge and the resonance stabilization concept is realized, and therefore this molecule qualifies as a "superbase".[5,6] The pK_a value of btmgn in CH_3CN was estimated to be 25.1 (experimentally derived estimate)[7] or 25.4 (calculated with the help of IPCM-B3LYP/6-311+G**//HF/6-31G* calculations and an empirical formula, IPCM = isodensity-polarized continuum model).[8,9] The protonated molecule (btmgn)H^+ was shown to establish (unsymmetric) imino N–H···N bridges,[4] a bonding situation characteristic for proton sponges. For comparison, in the protonated btmgb molecule (see Scheme 1), no such bridge is formed.[10]

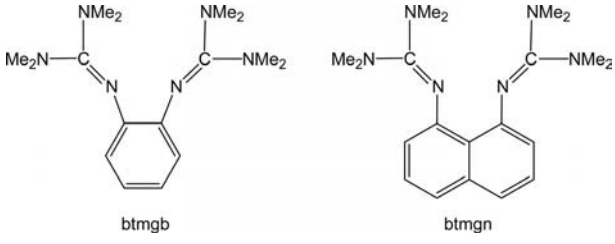

Scheme 1. Two GFA-2 ligands. Of these, btmgn represents a superbase.

Aromatic compounds functionalized with four or more guanidino groups (GFA-*n*, where *n* denotes the number of guanidino substituents) were recently introduced by us as a new class of strong organic electron donors and redox-active complex ligands.[11,12] Two representatives are 1,2,4,5-tetrakis(*N*,*N*,*N*′,*N*′-tetramethylguanidino)benzene (ttmgb, **1**)[11] and 1,2,4,5-tetrakis(*N*,*N*′-dimethyl-*N*,*N*′-ethyleneguanidino)benzene (tdmegb, **2**),[12] see Scheme 2. With an empirical formula provided by Maksić et al.,[13] the pK_a values of **1** and **2** were estimated to be 25.3 and 23.8, respectively, in CH_3CN solutions. The two-electron wave observed at $E_{1/2}(CH_3CN)$ = –0.32 V vs. SCE for **1** [11] shifts to –0.36 V for **2**.[12] Hence **2** is a slightly weaker Brønsted base than **1**, but a slightly superior electron donor in CH_3CN solution. Recent studies by our group revealed remarkable differences in the chemistry of **1** and **2**. For example **2**, but not **1**, was shown to assist C–H activation by Au^{I} complexes.[12] Another difference is the tendency of **1**, but not **2**, to decompose under amine elimination to give heterocycles.[14] Finally, variable-temperature NMR studies showed that the barrier for rotations around the N=C double bonds is smaller in **2** than in **1**, arguing for a carbenoid character of the heterocycle.[15]

[a] Anorganisch-Chemisches Institut, Ruprecht-Karls-Universität Heidelberg,
Im Neuenheimer Feld 270, 69120 Heidelberg, Germany
Fax: +49-6221-545707
E-mail: hans-jorg.himmel@aci.uni-heidelberg.de

Supporting information for this article is available on the WWW under http://dx.doi.org/10.1002/ejic.201001202.

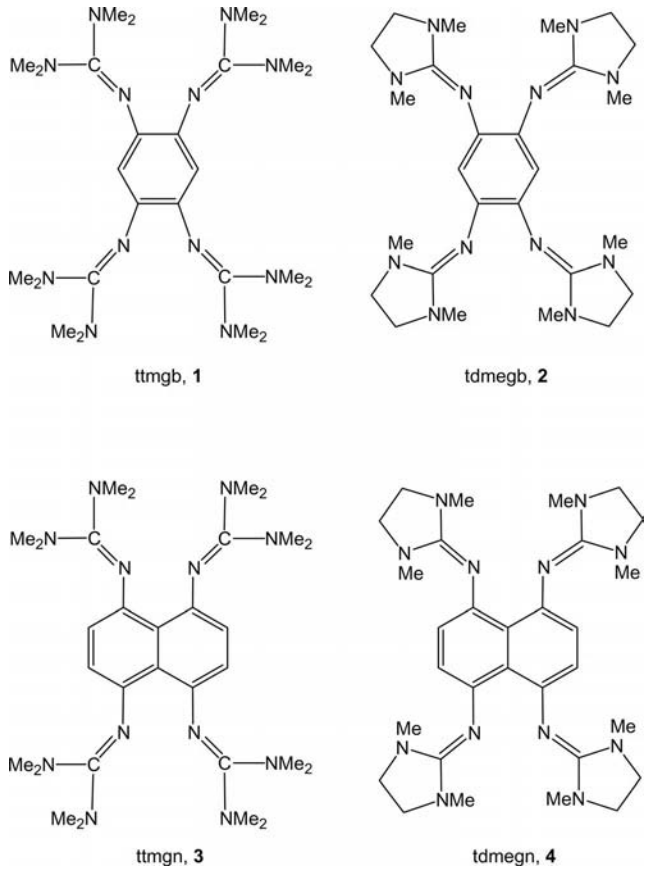

Scheme 2. Four representatives of strong organic GFA-4 electron donors and ligands. Of these, the synthesis and chemistry of **4** is described herein.

Recently we reported on the synthesis of the oxidation-labile and superbasic GFA-4 species 1,4,5,8-tetrakis(*N*,*N*,*N*′,*N*′-tetramethylguanidino)naphthalene (ttmgn, **3**), see Scheme 2.[16] Protonation experiments showed this molecule to be a double proton sponge. While **1** and **2** act as two-electron donors, **3** can be relatively easily oxidized either to the dication $\mathbf{3}^{2+}$, e.g. by I_2, or to the tetracation $\mathbf{3}^{4+}$, e.g. by Br_2. This has significant consequences for the redox chemistry of its coordination compounds, as shown herein. CV experiments found $E_{1/2}(CH_3CN) = -0.25$ V vs. SCE for $\mathbf{3}^{0/2+}$ and +0.50 V vs. SCE for $\mathbf{3}^{2+/4+}$.[16]

Attracted mainly by their high basicity, guanidines and guanidinates were used intensively in coordination chemistry,[17] and were found to establish strong σ(N→metal) and also π(N→metal) bonds.[18] In the last years, we synthesized a number of late transition metal complexes of the GFA-2 ligands btmgb and btmgn, (see Scheme 1).[18–20] Interestingly, Alder's proton sponge 1,8-bis(dimethylamino)naphthalene is barely suitable as ligand due to steric encumbrance at the amino N atoms. Up to date only a single example for a transition metal complex of this molecule is known.[21] In sharp contrast, we showed that the related bisguanidine btmgn (see Scheme 1) is a versatile ligand.[19] The metal ion in complexes of btmgn is often displaced considerably from the "best-plane" of the naphthyl backbone. For example, in [(btmgn)$PtCl_2$] the naphthyl backbone is curled and the Pt^{II} ion displaced by 133.1 pm from the naphthyl "best plane".[19] In additional work, the GFA-4 compound **1** was used for the synthesis of a variety of dinuclear metal complexes and also coordination polymers.[22–24] For example, ligand oxidation in the dinuclear Cu^{I} complex [**1**$(CuI)_2$] with I_2 was shown to give a semiconductive coordination polymer, [**1**$(CuI)_2](I_3)_2$, with a relatively low band gap (1.05 eV).[23]

Results and Discussion

Synthesis and Characterization of 4

Compound **4** was synthesized from 1,4,5,8-(tetraamino)-naphthalene and activated 1,3-dimethyl-2-imidazolidinone. The ^{1}H NMR spectrum in CD_3CN contains three singlet signals at δ = 2.55, 3.17 and 6.36 ppm due to the CH_3, CH_2 and aromatic CH protons, respectively. For comparison, the ^{1}H NMR spectrum of **3** (also in CD_3CN) features signals at δ = 2.66 (CH_3) and 6.02 ppm (aromatic CH).[16] The UV/Vis spectrum of **4** (see Figure 1, a) shows a broad absorption at 385 nm, which can be assigned to a transition involving the guanidino groups. The corresponding band for **3** was detected very close by at 393 nm.[16] Unfortunately

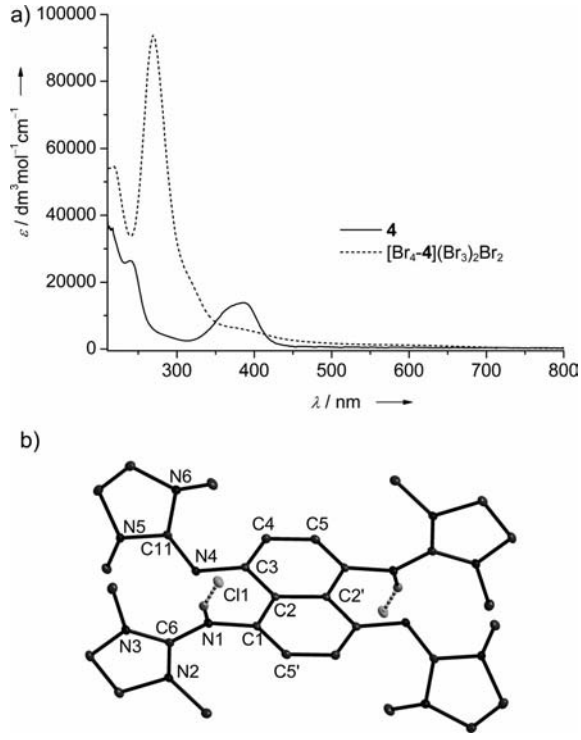

Figure 1. a) UV/Vis spectra of CH_3CN solutions of **4** and (Br_4-**4**)$(Br_3)_2Br_2$. b) Molecular structure of (**4**H_2)Cl_2 as derived from X-ray diffraction. Ellipsoids are drawn at the 50% probability level. Selected structural parameters (distances in pm, angles in deg): N1–C1 144.31(18), N1–C6 133.05(19), N2–C6 135.46(19), N3–C6 132.9(2), N4–C3 139.45(19), N4–C11 128.4(2), N5–C11 138.02(19), N6–C11 138.79(19), C1–C2 143.6(2), C1–C5′ 136.6(2), C2–C2′ 145.3(3), C2–C3 144.3(2), C3–C4 138.9(2), C4–C5 140.0(2), C1–N1–C6 128.26(13), N2–C6–N3 111.61(13), C3–N4–C11 123.76(12), N5–C11–N6 108.60(13).

all attempts to crystallize the neutral compound **4** failed. However, we were able to crystallize a salt of the diprotonated molecule, (**4**H_2)Cl_2, which is formed in the course of the synthesis (see Exp. Sect.). Its structure as determined by X-ray diffraction analysis is illustrated in Figure 1 (b). Protonation occurs exclusively at the imino N atoms, and the chloride anions are connected to the protonated GFA-4 via N–H···Cl contacts. Protonation leads to an increase in the N=C double bond length. Hence the bond length N1–C6 of 133.05(19) pm is significantly longer than the N4–C11 bond length [128.4(2) pm]. At the same time, the bond lengths N2–C6 and N3–C6 [135.46(19) and 132.9(2) pm] are considerably shorter than the bond lengths N5–C11 and N6–C11 [138.02(19) and 138.79(19) pm], signalling delocalization of the positive charge within the NCN_2 group of atoms.

Oxidation

In the CV curves recorded for **4** in CH_3CN solutions (see Figure 2 and Figure S1 in the Supporting Information), two two-electron waves appear at $E_{1/2}$ (CH_3CN) = –0.31 V (**4**/**4**$^{2+}$) and +0.56 V vs. SCE (**4**$^{2+}$/**4**$^{4+}$). In addition, some smaller features appear which might be due to a small amount of protonated molecules. We are currently analysing the possibility of CH_3CN deprotonation by **4**. Four electrons can be removed from the aromatic system of **4**. For comparison, $E_{1/2}$(CH_3CN) = –0.25 V and +0.50 V for ttmgn/ttmgn^{2+} and ttmgn^{2+}/ttmgn^{4+}.[16] Hence in CH_3CN solution, **4** appears to be a slightly better two-electron donor than **3**. This order in the electron donor capacity is in line with the results obtained for the pair **1** and **2**.[12] The organic electron acceptor TCNQ readily oxidizes **4** (removal of two electrons). A deep-green product is formed, which can be identified as the salt **4**$(TCNQ)_2$ (featuring formally the dication **4**$^{2+}$). The most intense signal in the mass spectrum can be assigned to **4**$^{2+}$. The UV/Vis spectra of CH_2Cl_2 solutions of the product (see Figure 3, a) immediately show the presence of [TCNQ]$^{-}$ radicals. Thus absorptions exhibiting vibrational fine structure typical for this radical,[25,26] show in the regions 650–900 and 350–500 nm. Unfortunately it proved impossible to grow crystals of this compound suitable for an XRD analysis. On the other hand, good-quality crystals of the corresponding salt of the electron donor **1** (see Scheme 2), **1**$(TCNQ)_2$ (also deep-green) were obtained from Me_2CO or CH_2Cl_2 solutions at –20 °C. Its UV/Vis spectrum is similar to that recorded for **4**$(TCNQ)_2$ (see Supporting Information). The structure is illustrated in Figure 3 (b). Most importantly, the radical anion units form dimeric units in the crystalline state.

Oxidation with the relatively strong inorganic electron acceptor Br_2 gives remarkably different results for **3** and **4**. In both cases, the GFA-4 molecules are oxidized to the +IV oxidation state. However, in the case of **4**, but not **3**, all four CH groups of the central C_{10} unit are replaced by CBr groups. The product, (Br_4-**4**)$(Br_3)_2Br_2$, crystallizes from CH_3CN solutions. Its molecular structure as derived from

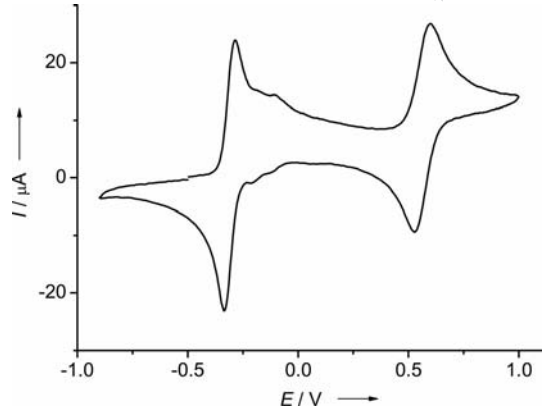

Figure 2. CV curve of **4** in CH_3CN solutions (SCE, scan speed 50 mV s^{-1}).

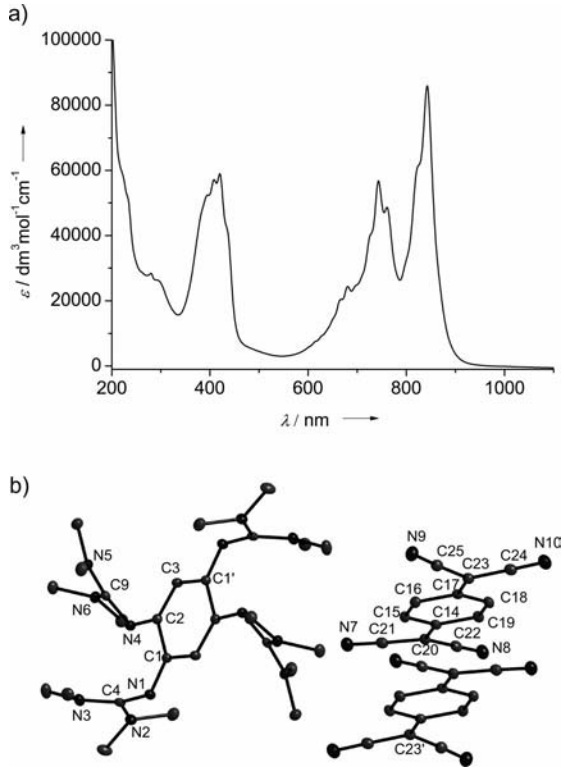

Figure 3. a) UV/Vis spectra recorded for **1**$(TCNQ)_2$ and **4**$(TCNQ)_2$ (CH_3CN solution). b) Molecular structure of **1**$(TCNQ)_2$ as derived from X-ray diffraction. Ellipsoids are drawn at the 50% probability level. Selected structural parameters (distances in pm, angles in deg): N1–C1 129.86(19), N1–C4 137.13(18), N2–C4 132.80(18), N3–C4 133.99(19), N4–C2 136.05(18), N4–C9 133.13(17), N5–C9 135.75(18), N6–C9 134.96(17), C1–C2 149.78(19), C2–C3 136.2(2), C3–C1′ 142.84(19), N7–C21 115.4(2), N8–C22 115.60(19), N9–C25 115.12(19), N10–C24 115.1(2), C20–C21 142.4(2), C20–C22 141.9(2), C23–C24 142.4(2), C23–C25 141.9(2), C14–C20 141.5(2), C17–C23 141.5(2), C14–C15 142.1(2), C15–C16 136.8(2), C16–C17 141.6(2), C17–C18 142.2(2), C18–C19 136.4(2), C14–C19 142.3(2), C20···C23′ 327.9(65), C1–N1–C4 126.32(12), C2–N4–C9 123.03(12).

an XRD analysis is illustrated in Figure 4. The side-view shown in part b of Figure 4 highlights the curled form of the central $C_{10}Br_4$ unit. The C–C bond lengths within the

central C_{10} unit vary within the range 132.6(2) (C2–C3) and 151.4(2) (C1–C2) pm. The C1–N1 and C4–N4 bond lengths measure 129.2 and 131.5 pm and are shorter than the distances N1–C11 and N4–C16 of 138.8 and 135.0 pm (which were N=C double bonds before oxidation). Hence each of the two guanidino groups on the "right side" in the molecular structure shown in Figure 4 carries formally one positive charge, which is delocalized within the N2–C11–N3 and N5–C16–N6 groups of atoms. On the other hand, the two guanidino units on the "left side" of the structure in Figure 4 exhibit significantly different bonding parameters. With 140.1 and 143.2 pm, the N7–C6 and N10–C9 bond lengths are much longer than the N1–C1 and N4–C4 bond lengths, and consequently the N7–C21 and N10-C26 bond lengths (133.1 and 132.3 pm) remain relatively short. This leads to the conclusion that formally only two guanidino groups (in para position to each other) are oxidized. The two remaining positive charges seem to be delocalized within some of the C atoms of the central C_{10} ring. This situation is in sharp contrast to that found in (**3**)Br_4, for which all four guanidino groups are virtually identical.[16] To obtain more information, quantum chemical calculations were carried out for the free tetracation $(Br_4\text{-}\mathbf{4})^{4+}$. The calculated gas-phase values for the free tetracation are compared to the experimentally derived ones in Table S1 (see Supporting Information). According to the calculations the four guanidino groups in the free tetracation exhibit equal bond parameters. The four bond lengths N1–C1, N4–C4, N7–C6, and N10–C9 all measure 127.8 pm, and are thus shorter than the bond lengths N1–C11, N4–C16, N7–C21, and N10-C26 (all 137.9 pm). It can be concluded that polarization effects are likely to be responsible for the unusual geometry in the salt $(Br_4\text{-}\mathbf{4})(Br_3)_2Br_2$. The UV/Vis spectrum of $(Br_4\text{-}\mathbf{4})(Br_3)_2Br_2$ in a CD_3CN solution is included in Figure 1. It is dominated by a strong band at 269 nm, which can be assigned to the Br_3^- anion.[27] This band slowly decays with time due to decomposition in solution to give Br_2 and Br^-. Most importantly, the band at 385 nm characteristic for neutral **4** disappeared completely, signalling a massive change in the electronic structure upon oxidation.

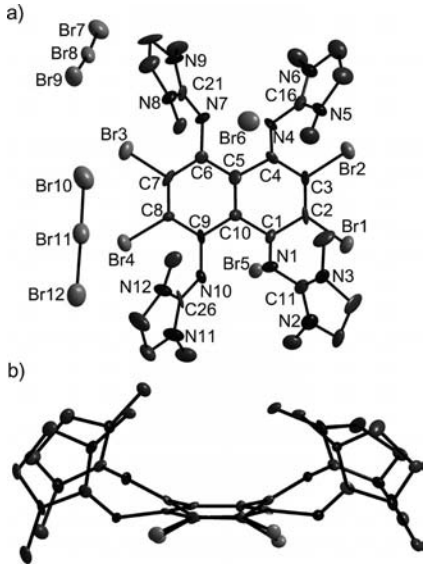

Figure 4. Molecular structure of $(Br_4\text{-}\mathbf{4})(Br_3)_2Br_2$ as derived from X-ray diffraction. Ellipsoids are drawn at the 50% probability level. Selected structural parameters (distances in pm, angles in deg): N1–C1 129.2(16), N1–C11 138.8(16), N2–C11 136.4(17), N3–C11 134.6(17), N4–C4 131.5(14), N4–C16 135.0(15), N5–C16 134.5(15), N6–C16 133.1(17), N7–C6 140.1(15), N7–C21 133.1(15), N8–C21 130.5(17), N9–C21 134.3(16), N10–C9 143.2(15), N10–C26 132.3(14), N11–C26 134.0(18), N12–C26 131.4(16), C2–Br1 187.8(12), C3–Br2 187.6(11), C7–Br3 188.4(11), C8–Br4 189.3(11), C1–C2 151.4(15), C1–C10 147.3(15), C2–C3 132.6(17), C3–C4 144.2(16), C4–C5 150.7(16), C5–C6 141.1(16), C5–C10 134.7(18), C6–C7 140.8(17), C7–C8 137.2(18), C8–C9 138.5(15), C9–C10 145.2(15), Br7–Br8 247.8(3), Br8–Br9 255.2(3), Br10–Br11 246.7(3), Br11–Br12 263.1(3), C1–N1–C11 125.1(11), C4–N4–C16 126.7(11), C6–N7–C21 124.7(10), C9–N10–C26 124.3(9), N2–C11–N3 113.2(11), N5–C16–N6 112.4(11), N8–C21–N9 112.6(11), N11–C26–N12 112.8(11), Br7–Br8–Br9 175.47(10), Br10–Br11–Br12 176.97(9).

Oxidation of **4** with the weaker electron acceptor I_2 gave no clear results, in contrast to the reaction between **3** and I_2 [which gave **3**$(I_3)_2$].[16] A small number of crystals were grown from a solution containing **4** and I_2, representing a product of a side reaction, which nevertheless turned out to be of interest. The analysis of the XRD data showed the product to be the hydrated salt $[C_{60}H_{88}N_{24}]I_6 \cdot 4.5H_2O$, composed of two tetraguanidino units (see Scheme 3 and Supporting Information). The protons required for protonation of two of the guanidino groups are released in the course of C–C bond formation between the two C_{10} rings. It is not yet clear how this product is formed, especially in the light of the necessary movement of two guanidino groups (from position 1 to 2 in the C_{10} ring).

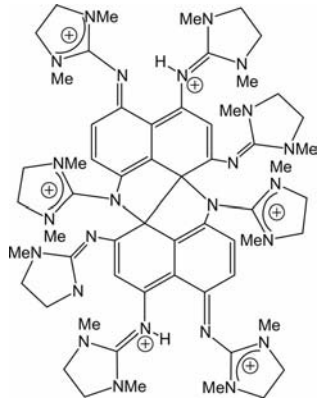

Scheme 3.

Coordination Chemistry

In the following we report on some aspects of the coordination chemistry of the two ligands **3** and **4**. The synthesis of the two dinuclear Co^{II} complexes [**3**$(CoCl_2)_2$][16] and [**4**$(CoCl_2)_2$] allows to compare structural details and also the magnetism of simple complexes of these two ligands. Furthermore, Ni^{II} and Cu^{I} complexes of **3** were synthesized and analysed. Finally, oxidation of the dinuclear Cu^{I} complexes with Br_2 was investigated.

Co and Ni Complexes: The new compound **4** was brought to reaction with $CoCl_2$ to give the dinuclear complex [**4**$(CoCl_2)_2$]. Crystals of this complex were grown at –18 °C from CH_3CN solutions layered with Et_2O. The molecular structure as derived from an XRD study is illustrated in Figure 5. It can be seen that the molecules adopt a *boat*-type conformation in the crystalline state, in contrast to the *chair*-type arrangement found for the corresponding complex of **3**, [**3**$(CoCl_2)_2$].[16] As a consequence, the Co···Co separation in [**4**$(CoCl_2)_2$] (772.9 pm) is shorter than the Co···Co separation in [**3**$(CoCl_2)_2$] (795.2 pm).[16] All the other structural data are quite similar. Hence Co–N bond lengths of 198.0(4) and 198.4(6) pm in [**4**$(CoCl_2)_2$] compare with 199.6(2) pm in [**3**$(CoCl_2)_2$].[16] The N–Co–N and Cl–Co–Cl bond angles measure 88.0(2)° and 111.63(7)° in [**4**$(CoCl_2)_2$] and 87.8(1)° and 116.6(1)° in [**3**$(CoCl_2)_2$]. The UV/Vis spectrum of [**4**$(CoCl_2)_2$] is compared to that of free **4** as shown in part a of Figure 6. It features a broad and strong absorption centered at 407 nm. In addition, two weak features show at 611 and 686 nm, together with a shoulder at ca. 570 nm (see Figure 6, b), which can be assigned to d-d transitions.

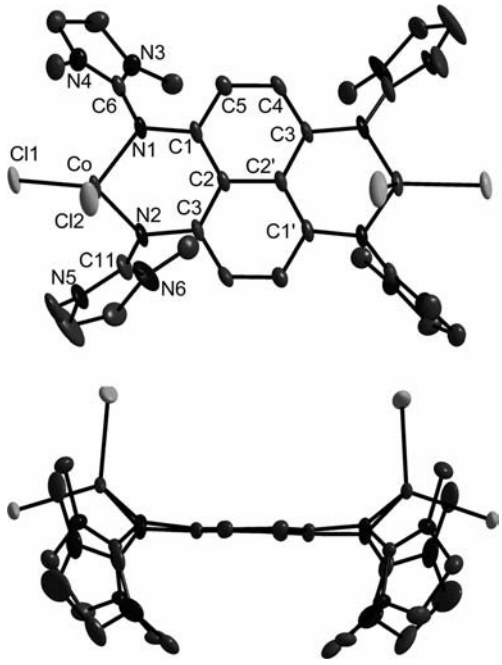

Figure 5. Molecular structure of [**4**$(CoCl_2)_2$] as derived from X-ray diffraction. Ellipsoids are drawn at the 20% probability level. Selected structural parameters (distances in pm, angles in deg): Co–N1 198.0(4), Co–N2 198.4(6), Co–Cl1 227.29(17), Co–Cl2 225.5(2), N1–C1 141.2(6), N1–C6 132.9(7), N2–C3 143.7(6), N2–C11 130.4(9), N3–C6 134.1(7), N4–C6 132.7(7), N5–C11 136.5(8), N6–C11 133.9(11), C1–C2 142.7(8), C1–C5 138.7(8), C2–C2′ 146.1(9), C2–C3 142.4(8), C2′–C3′ 142.4(8), C3′–C4 137.1(8), C4–C5 139.3(8), N1–Co–N2 88.0(2), Cl1–Co–Cl2 111.63(7), C1–N1–Co 120.7(4), C1–N1–C6 119.4(4), C3–N2–Co 117.6(4), C3–N2–C11 118.2(6), N3–C6–N4 110.1(5), N5–C11–N6 109.2(7).

The three dinuclear Ni^{II} complexes [**3**$(NiX_2)_2$], with X = Cl, Br and acac, were synthesized by reaction between **3** and the dme complexes of $NiCl_2$ and $NiBr_2$, or between **3** and $Ni(acac)_2$. Unfortunately all attempts to obtain crystals

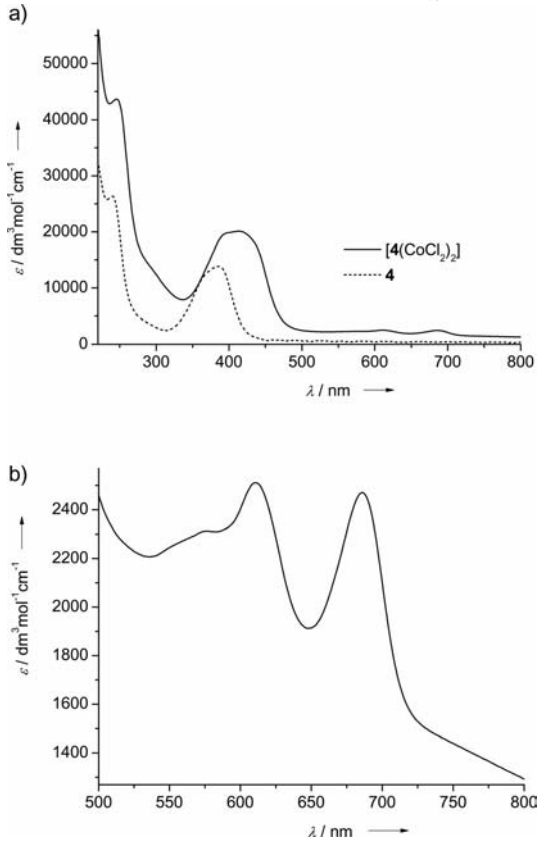

Figure 6. a) UV/Vis spectrum of [**4**$(CoCl_2)_2$] in CH_3CN solution together with that of free tdmegn. b) The region 500–800 nm showing bands due to d-d transitions.

suitable for X-ray diffraction for at least one of the three complexes failed. Quantum chemical (B3LYP/SVP) calculations were therefore carried out to obtain some insight into the likely structure of [**3**$(NiCl_2)_2$] (see Supporting Information). These calculations found a *trans*-type coordination geometry, and four similar Ni–N bond lengths of 210.6 pm length. The N–Ni–N and Cl–Ni–Cl bond angles measure 86.5° and 135.3°, respectively.

Finally the magnetism was studied by SQUID measurements for solid samples of all five dinuclear Co and Ni complexes. Magnetization data were collected at an applied field of 0.5, 1, 2, 3, 4 and 5 T and corrected for the underlying diamagnetism. The results together with curve fits accomplished with the aid of the JulX program package[28] are included in Figures 7, 8 and 9. The simulations are based on the following spin-Hamiltonian operator as shown below.

$$\hat{H} = g\beta\hat{\vec{S}}\cdot\vec{B} + D\left(\hat{S}_z^2 - \frac{1}{3}S(S+1) + E/D(\hat{S}_x^2 - \hat{S}_y^2)\right)$$

Table 1 includes the parameters used for the curve fitting for all complexes. The magnetic coupling constant J came out to be very small ($<10\ cm^{-1}$) in all cases. The axial zero-field splitting parameter ($D_1 = D_2$) is small ($\leq 7\ cm^{-1}$) in the octahedral complexes {with [Ni(acac)$_2$]}, and reaches a

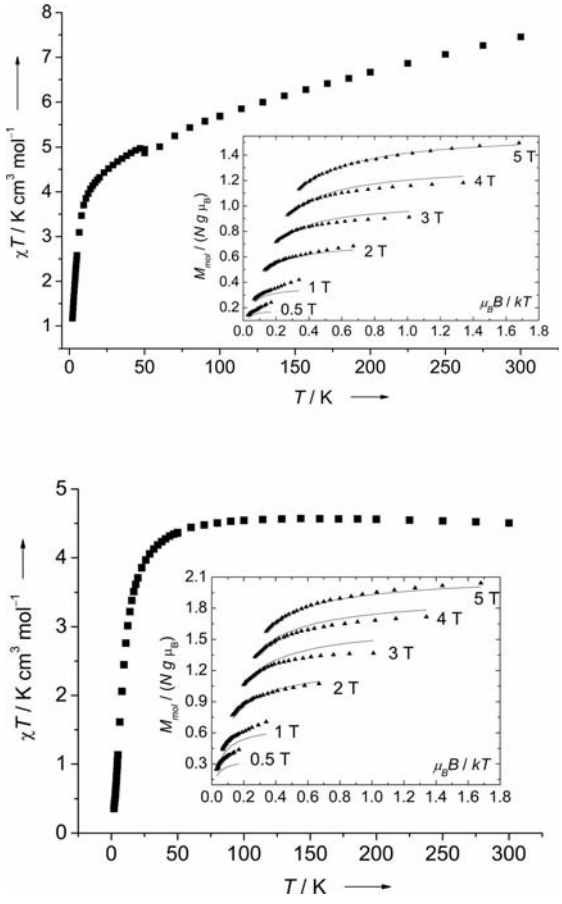

Figure 7. $\chi T-T$ curve as derived from SQUID measurements for a) [**4**$(CoCl_2)_2$] and b) [**3**$(CoCl_2)_2$], together with the temperature dependence of the molar magnetization at B = 0.5, 1, 2, 3, 4 and 5 T sampled on a $1/T$ inverse temperature scale (inset). The solid lines are the result of a global spin Hamiltonian simulation (see text).

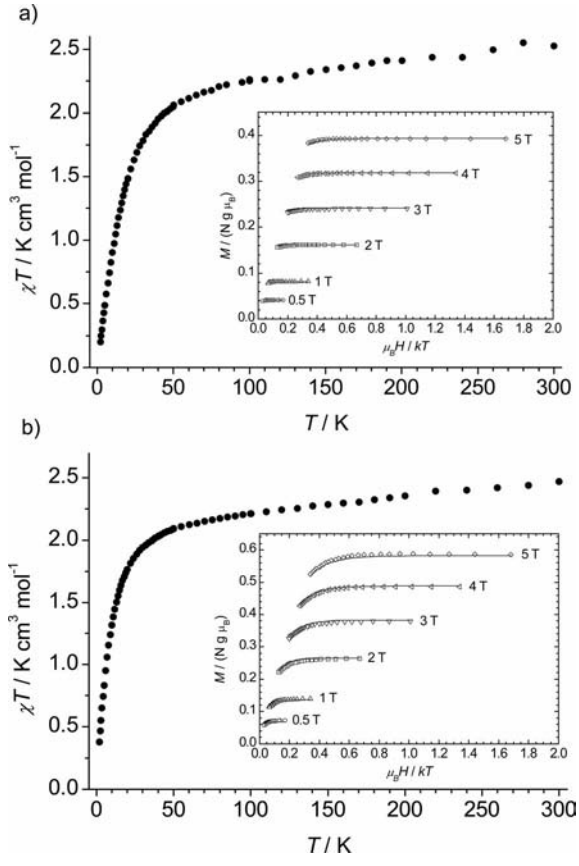

Figure 8. $\chi T-T$ curve as derived from SQUID measurements for a) [**3**$(NiCl_2)_2$], and b) [**3**$(NiBr_2)_2$], together with the temperature dependence of the molar magnetization at B = 0.5, 1, 2, 3, 4 and 5 T sampled on a $1/T$ inverse temperature scale (inset). The solid lines are the result of a global spin Hamiltonian simulation (see text).

maximum of 46 cm^{-1} in the tetrahedral complex [**3**$(NiBr_2)_2$].

Cu^I Complexes and Their Oxidation: Reaction between **3** and two equivalents of CuBr in CH_3CN at 70 °C yielded the new dinuclear Cu^I complex [**3**$(CuBr)_2$], which precipitated from the reaction mixture in the form of green, plate-like crystals. Its molecular structure as derived from XRD studies is displayed in Figure 10. The metal ions are again significantly displaced from the ligand aromatic plane (by 78.2 pm). Similar displacements were observed previously for coordination compounds involving btmgn[19] and **3**[16] (see Scheme 1 and Scheme 2). The sum of structural data now available for btmgn and **3** show that the displacement of metal ions generally increases from tetrahedral via trigonal planar to square-planar coordination geometries, reflecting the steric constrains imposed by the tetramethylguanidino groups. For example, the metal ions in the complexes [(btmgn)$PdCl_2$] and [(btmgn)$PtCl_2$] (both almost planar geometries) are displaced by 133.8 and 133.1 pm, respectively, from the ligand naphthalene ring plane.[19] The adjacent tetraguanidino groups in [**3**$(CuBr)_2$] adopt a *cis*-type conformation. In an analogue reaction, involving CuI

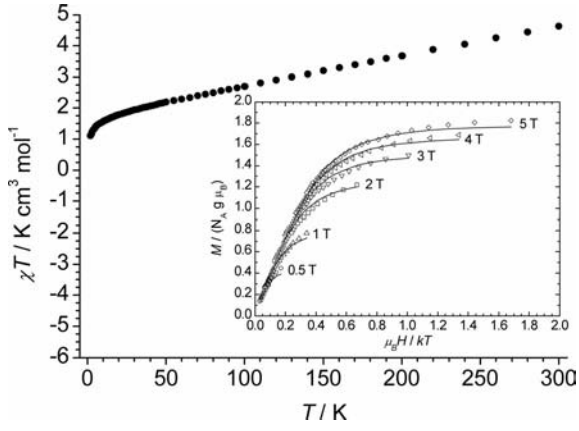

Figure 9. $\chi T-T$ curve as derived from SQUID measurements for [**3**$(Ni(acac)_2)_2$], together with the temperature dependence of the molar magnetization at B = 0.5, 1, 2, 3, 4 and 5 T sampled on a $1/T$ inverse temperature scale (inset). The solid lines are the result of a global spin Hamiltonian simulation (see text).

in place for CuBr, the complex [**3**$(CuI)_2$] was synthesized. We again obtained a crystal structure of this complex, which is illustrated in Figure 11. As anticipated, the Cu^I ions in [**3**$(CuI)_2$] are displaced from the ligand ring plane

Table 1. Comparison between the parameters derived from an analysis of the SQUID data for all known dinuclear Co^{II} and Ni^{II} complexes of **1**,[a] **3** and **4**. (c.n.: coordination number).

Ligand		$CoCl_2$ (c.n. 4)	$NiCl_2$ (c.n. 4)	$NiBr_2$ (c.n. 4)	$Ni(acac)_2$ (c.n. 6)
1	$g_1 = g_2$	2.12	2.09	2.09	2.20
	J [cm^{-1}]	2.73	0.68	0.48	–0.04
	$D_1 = D_2$ [cm^{-1}]	16.0	30.3	33.1	4.4
	$E/D_1 = E/D_2$	0.09	0.33	0.50	0.00
	θ_{CW} [K]	–1.56	0.01	0.09	0.09
	TIP [10^{-6} $cm^3 mol^{-1}$]	0.5	0.1	30.3	1.2
3	$g_1 = g_2$	2.55	2.02	2.13	2.18
	J [cm^{-1}]	7.90	–0.03	1.91	2.52
	$D_1 = D_2$ [cm^{-1}]	19.5	34.7	46.2	7.0
	$E/D_1 = E/D_2$	0.30	0.33	0.61	0.00
	θ_{CW} [K]	–10.0	0.05	0.02	–0.48
	TIP [10^{-6} $cm^3 mol^{-1}$]	2.0	0.4	0.1	0.0
4	$g_1 = g_2$	2.50	–	–	–
	J /cm^{-1}	4.60			
	$D_1 = D_2$ [cm^{-1}]	21.0			
	$E/D_1 = E/D_2$	0.00			
	θ_{CW} [K]	–18.4			
	TIP [10^{-6} $cm^3 mol^{-1}$]	60.0			

[a] Fit parameters were taken from ref.[27]

(also by 78.2 pm), and the tetramethylguanidino groups on each side of the naphthalene plane again adopt *cis*-conformation.

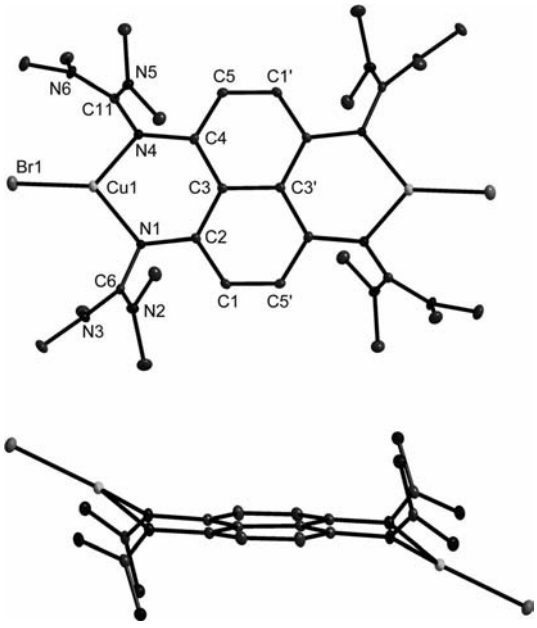

Figure 10. Molecular structure of [**3**$(CuBr)_2$]. Thermal ellipsoids drawn at the 50% probability level. Selected structural parameters (bond lengths in pm, bond angles in deg): Cu1–Br1 230.41(9), Cu1–N1 199.31(16), Cu1–N4 201.71(18), N1–C2 141.4(2), N1–C6 133.4(2), N2–C6 137.2(3), N3–C6 135.1(3), N4–C4 142.4(3), N4–C11 132.3(3), N5–C11 136.4(3), N6–C11 136.7(3), C1–C2 138.2(3), C1–C5′ 138.4(3), C2–C3 144.0(3), C3–C3′ 147.1(4), C3–C4 144.6(3), C4–C5 137.8(3), N1–Cu1–Br1 134.69(5), N4–Cu1–Br1 135.68(5), C2–N1–Cu1 123.34(13), C2–N1–C6 116.19(16), C4–N4–Cu1 123.18(13), C4–N4–C11 118.42(17).

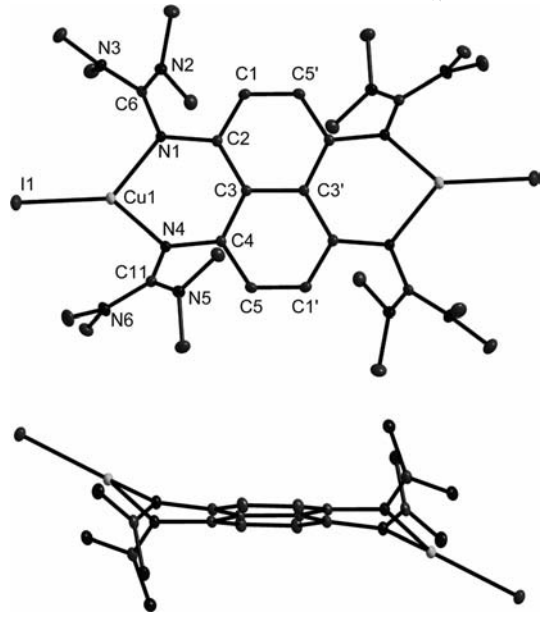

Figure 11. Molecular structure of [**3**$(CuI)_2$]. Thermal ellipsoids drawn at the 50% probability level. Selected structural parameters (bond lengths in pm, bond angles in deg): Cu1–I1 245.69(10), Cu1–N1 199.50(14), Cu1–N4 200.56(14), N1–C2 141.6(2), N1–C6 132.7(2), N2–C6 137.0(2), N3–C6 135.3(2), N4–C4 142.50(19), N4–C11 132.4(2), N5–C11 136.4(2), N6–C11 136.8(2), C1–C2 138.3(2), C1–C5′ 138.6(2), C2–C3 143.7(2), C3–C3′ 147.2(3), C3–C4 144.8(2), C4–C5 137.6(2), N1–Cu1–I1 131.87(4), N4–Cu1–I1 137.93(4), C2–N1–Cu1 123.74(10), C2–N1–C6 116.57(13), C4–N4–Cu1 121.28(10), C4–N4–C11 117.91(13).

Subsequently, oxidation of [**3**$(CuBr)_2$] by Br_2 was studied. The results show that reaction proceeds according to Equation (1) to give the salt **3**$[CuBr_4]_2$. In Figure 12 the structure obtained by XRD is visualized. In this salt direct bonds between the oxidized **3** and the metal ions are absent.

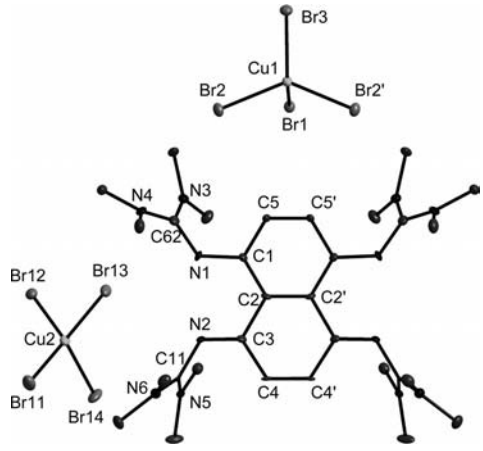

Figure 12. Molecular structure of **3**$[CuBr_4]_2$. Thermal ellipsoids drawn at the 50% probability level. Selected structural parameters (bond lengths in pm, bond angles in deg): Cu1–Br1 237.17(14), Cu1–Br2 240.47(8), Cu1–Br3 236.79(14), Cu2–Br11 235.90(12), Cu2–Br12 239.66(11), Cu2–Br13 239.63(10), Cu2–Br14 235.31(11), N1–C1 140.2(7), N1–C62 136.6(8), N2–C3 127.6(8), N2–C11 138.6(8), C1–C2 140.3(8), C1–C5 141.8(8), C2–C3 152.1(8), C3–C4 145.5(8), C4–C4′ 133.6(11), C5–C5′ 136.7(11).

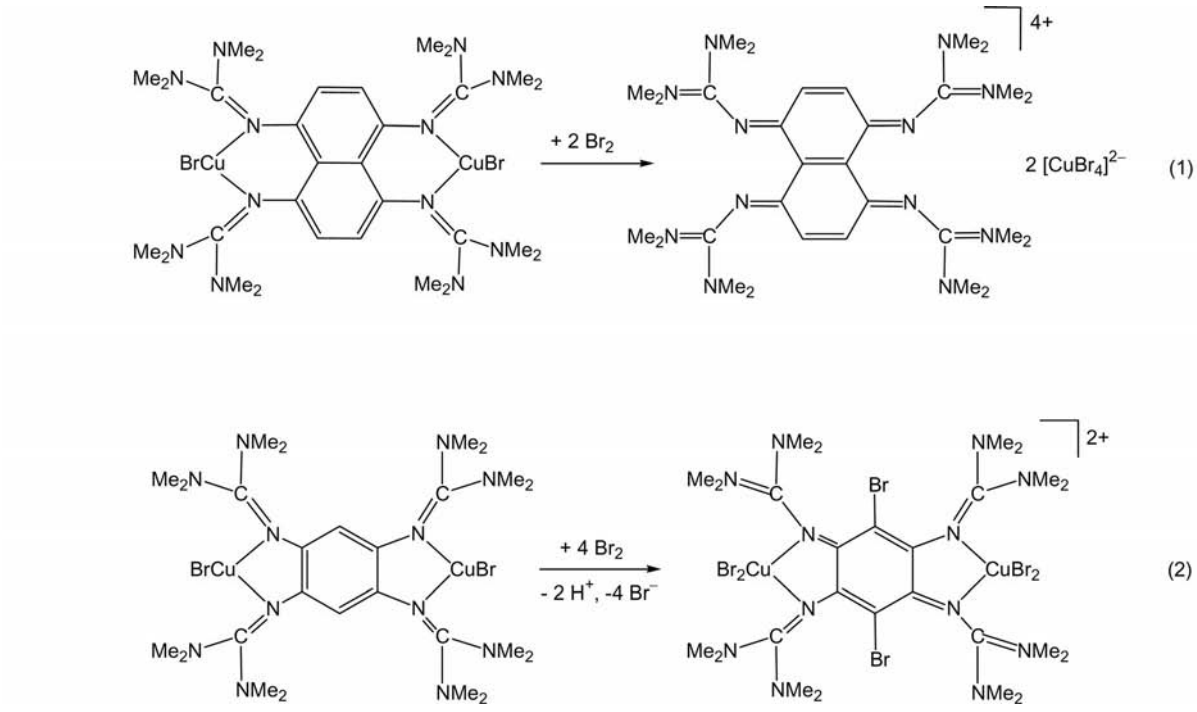

Hence four-electron oxidation of **3** occurs and the Cu^{I} ions are oxidized to Cu^{II}. This behaviour is in clear contrast to that observed for reaction between [**1**$(CuBr)_2$] and Br_2, which leads to the dinuclear Cu^{II} complex [$(Br_2$-**1**$)(CuBr_2)_2]^{2+}$ with intact Cu–N bonds as shown in Equation (2).[23] While four electrons can be removed from **3**, compound **1** offers only two electrons. Due to the strong basicity of guanidines, **1** and **2** are still able to act as ligands upon two-electron oxidation. However, with further removal of two electrons as observed for **3** and **4**, the guanidino-metal interactions become too weak, and a salt is formed.

Conclusions

In this work we evaluated in detail the chemistry of the redox-active compounds **3** and the newly synthesized **4**. CV measurements indicate that **4** is a slightly better electron donor than **3** in CH_3CN solutions. Both compounds can be oxidized relatively easily to the dication or tetracation, in dependence of the strength of the oxidation agent. However, reaction with an excess of the electron acceptor Br_2 leads to different products. Hence reaction with **3** leads simply to removal of four electrons and formation of the salt (**3**)Br_4; reaction with **4** leads in addition to bromination of the C_{10} central unit to give (Br_4-**4**)$(Br_3)_2Br_2$. Several dinuclear transition metal complexes were prepared and structurally analysed. The magnetism in dinuclear Co^{II} and Ni^{II} complexes with different coordination modes was studied with the aid of SQUID measurements. The magnetic coupling in all complexes turned out to be weak. The axial zero-field splitting parameter varies considerably for different coordination modes. Removal of four electrons from the ligand unit in dinuclear Cu^{I} complexes of **3** leads to cleavage of the Cu-guanidine coordination bond. Future experiments will concentrate on the isolation of coordination compounds with the dications of **3** and **4**, which should still establish relatively strong coordination bonds with metal ions. In the same way as shown already for **1**,[23] it should then be possible to synthesize coordination polymers with interesting electronic properties (for instance, electric conductivity).

Experimental Section

General: All reactions were carried out under inert gas atmosphere using standard Schlenk techniques. The preparation of **3** was already previously reported by us.[13] For the SQUID direct current (dc) measurements, a Quantum Design MPMS-XL 5 was used. IR and UV/Vis measurements were carried out on a BioRad Merlin Excalibur FT 3000 and a Perkin–Elmer Lambda 19 machine, respectively. Infrared spectra were recorded using a BIORAD Excalibur FTS 3000. NMR spectra were taken on a Bruker Avance II 400 or on a Bruker Avance DPX AC200. Elemental analyses were carried out at the Microanalytical Laboratory of the University of Heidelberg. EI mass spectra were obtained on a Finnigan MAT 8230 or on a JEOL JMS-700 instrument. A EG&G Princeton 273 apparatus was used for the CV measurements.

4: 1,5-Dinitronaphthalene (4.90 g, 22.5 mmol) was added to a solution of fuming nitric acid (14 mL) and concentrated sulfuric acid (12.5 mL). The reaction mixture was kept at a temperature of 20 °C during the addition. Subsequently, it was slowly heated to 80 °C and kept at this temperature for a period of 2 h. After cooling the

solution to 5 °C, it was filtered to give a mixture of the two isomers 1,4,5,8- and 1,3,5,8-tetranitronaphthalene. 1,4,5,8-Tetranitronaphthalene was separated from its isomer by filtration from hot ethanol and then recrystallized from acetone. Yield of 1,4,5,8-tetranitronaphthalene: 1.814 g (52.4%). ^{1}H NMR (199.92 MHz, [D$_6$]DMSO): δ = 8.83 (s). Then a suspension of 1,4,5,8-tetranitronaphthalene (1.814 g, 5.90 mmol) in ethanol (60 mL) was added to a solution of $SnCl_2$ (22.4 g, 11.8 mmol, 20 equiv.) dissolved in concentrated HCl (90 mL). The mixture was stirred for 2.5 h at 40 °C. The volume of the mixture was subsequently condensed to 100 mL. The product precipitated from this solution. The solution was filtered off and the product dried under vacuum. Yield of 1,4,5,8-tetraaminonaphthalene complexed with $SnCl_2$ (denoted tetraamino salt hereafter): 2.27 g (86.2%). ^{1}H NMR (199.92 MHz, [D$_6$]DMSO): δ = 4.422 (s), 6.847–7.357. 1,3-dimethyl-2-imidazolidinone (3 mL, 27.9 mmol) was dissolved in 12 mL of dry $CHCl_3$ and oxalyl chloride (12 mL, 139.5 mmol) was added drop wise to this solution. The reaction mixture was stirred for 16 h under reflux under an inert atmosphere. After removal of the solvent under vacuum the product of the reaction was washed with Et_2O (40 mL), then dissolved in 50 mL of CH_3CN and added slowly and drop wise to 30 mL of a CH_3CN solution containing 2.50 g (5.59 mmol) of the tetraamino salt and 5.0 mL (36.2 mmol) of triethylamine at –10 °C. After stirring the mixture for 2 h at –10 °C, the solvent was removed under vacuum. The precipitate was re-dissolved in 10% HCl (15 mL) and an excess of 25% NaOH (40 mL) was added whilst stirring to deprotonate the product. Subsequently the product of the reaction precipitated from this solution, immediately was filtered off under an inert atmosphere, washed with CH_3CN and dried under vacuum yielding **4** as yellow powder; yield 0.359 g (0.63 mmol, 11.3%). $C_{30}H_{44}N_{12}$ (572.86): calcd. C 62.89, H 7.76, N 29.35; found C 62.01, H 7.57, N 28.38. ^{1}H NMR (399.89 MHz, CD_3CN): δ = 2.55 (s, 24 H, CH_3), 3.17 (s, 16 H, CH_2), 6.36 (s, 4 H) ppm. ^{13}C NMR (100.56 MHz, CD_3CN): δ = 154.53, 141.30, 125.93, 117.45 (CH), 48.63 (CH_2), 34.75 (CH_3) ppm. IR (CsI): $\tilde{\nu}$ = 2943 (w), 2846 (w), 1663 (vs), 1588 (s), 1559 (s), 1481 (s), 1433 (s 1384vs), 1277 (vs), 1240 (vs), 143 (w), 1073 (w), 1036 (s), 980 (m), 932 (w), 902 (m), 835 (m), 689 (m), 664 (w), 631 (w), 572 (w) cm^{-1}. UV/Vis (CH_3CN, $c = 1.09\times10^{-4}$ mol L^{-1}): λ_{max} (ε in dm^{3}mol^{-1}cm^{-1}) = 385 (1.37×10^4), 240 (2.62×10^4) nm. MS (ESI): *m*/*z* (%) = 287.2 (100) [**4**H$_2$]$^{2+}$, 573.4 (80) [**4**H]$^+$.

(4H$_2$)Cl$_2$: The salt was formed in the course of the synthesis of neutral **4**. ^{1}H NMR (399.89 MHz, CD_3CN): δ = 2.74 (s, 24 H, CH_3), 3.57 (s, 16 H, CH_2), 6.76 (s, 4 H), 13.34 (s, 2 H) ppm. IR (CsI): $\tilde{\nu}$ = 3587 (m), 3414 (m), 3236 (w), 3139 (w), 2891 (w), 1642 (s), 1581 (m), 1490 (m), 1389 (s), 1281 (s), 1199 (m), 1080 (m), 1042 (s), 984 (m), 941 (m), 910 (s), 803 (s), 699 (m, 85m), 644 (m), 557 (m), 495 (m), 427 (m) cm^{-1}. Crystal data for $C_{30}H_{46}Cl_2N_{12}$: *M*r = 645.69, $0.30\times0.25\times0.25$ mm^3, triclinic, space group $P\bar{1}$, *a* = 8.1320(16), *b* = 8.1430(16), *c* = 12.737(3) Å, *α* = 100.72(3)°, *β* = 93.51(3)°, *γ* = 102.61(3)°, *V* = 804.2(3) Å^3, *Z* = 1, d_{calc} = 1.333 Mg m^{-3}, Mo-K_α radiation (graphite-monochromated, λ = 0.71073 Å), *T* = 100 K, θ_{range} 2.58 to 30.04°. Reflections measd. 8346, indep. 4663, R_{int} = 0.0317. Final *R* indices [$I>2\sigma(I)$]: R_1 = 0.0464, wR_2 = 0.1079.

4(TCNQ)$_2$: 0.0214 g (0.104 mmol) TCNQ in 5 mL CH_3CN were added to a suspension of 0.0300 g (0.052 mmol) of **4** in 10 mL CH_3CN. The solution immediately turned to a deep-green colour. The mixture was stirred for 30 min at room temp. Subsequently the solvent was removed until 5 mL were left. The product of the reaction precipitated from this solution in three days as a dark-green powder which was washed with Et_2O and dried in vacuo; yield 0.024 g (0.024 mmol, 47.0%). $C_{54}H_{52}N_{20}$ (981.26): calcd. C 66.09, H 5.35, N 28.56; found C 65.98, H 5.28, N 28.45. MS (ESI %): *m*/*z* (%) = 286.3 (100) [**4**]$^{2+}$, 572.4 (10) [**4**]$^+$. UV/Vis (CH_3CN, $c = 1.98\times10^{-5}$ mol L^{-1}): λ_{max} (ε in dm^{3}mol^{-1}cm^{-1}) = 842 (0.85×10^5), 760 (0.49×10^5), 743 (0.57×10^5), 682 (0.24×10^5), 412 (0.56×10^5), 282 (0.28×10^5) nm. IR (CsI): $\tilde{\nu}$ = 2943 (w), 2974 (w), 2176 (vs), 1638 (s), 1600 (vs), 1546 (s), 1512 (m), 1458 (w), 1413 (w), 1352 (m), 1290 (w), 1233 (m), 1172 (s), 1039 (m), 974 (w), 932 (w), 817 (w), 787 (w), 699 (w), 668 (w), 642 (w), 504 (w) cm^{-1}.

1(TCNQ)$_2$: A solution of 7,7,8,8-tetracyanoquinodimethane (86 mg, 0.42 mmol) in toluene (40 mL) was slowly added via syringe to a solution of **1** (110 mg, 0.21 mmol) in toluene (10 mL) under argon atmosphere. The reaction mixture was stirred for 1 h at room temp., during which time a dark-green precipitate was observed. Then the precipitate was filtered off and dried under vacuum leading to 0.188 g (0.20 mmol, 97%) of **1**(TCNQ)$_2$ as a dark-green powder. m.p. 179–180 °C. $C_{50}H_{58}N_{20}$ (939.15): calcd. C 63.95, H 6.22, N 29.83; found C 64.68, H 5.54, N 29.01. IR (CsI): $\tilde{\nu}$ = 2927 (w), 2652 (w), 2175 (s), 2156 (m), 1590 (vs), 1500 (vs), 1465 (vs), 1418 (vs), 1397 (vs), 1364 (vs), 1314 (vs), 1273 (s), 1261 (s), 1230 (m), 1175 (vs), 1139 (m), 1062 (m), 1018 (vs), 986 (w), 984 (w), 897 (w), 862 (m), 827 (m), 752 (s), 718 (m), 691 (m), 619 (m), 583 (m), 541 (m), 482 (m) cm^{-1}. MS (ESI$^-$): *m*/*z* (%) = 204 (100) [TCNQ]$^-$. MS (FAB$^+$): *m*/*z* (%) = 532 (100) [**1**H$_2$]$^+$, 486 (51) [**1** – N(CH$_3$)$_2$]$^+$. UV/Vis (CH_2Cl_2, $c = 2.9\times10^{-5}$ mol L^{-1}): λ_{max} (ε in dm^{3}mol^{-1}cm^{-1}) = 302 (1.26×10^4), 409 (7.63×10^4), 423 (7.90×10^4), 671 (1.36×10^4), 685 (1.61×10^4), 750 (4.55×10^4), 767 (3.93×10^4), 852 (1.03×10^5) nm. Crystal data for **1**(TCNQ)$_2\times2$Me$_2$CO, $C_{56}H_{70}N_{20}O_2$: *M*r = 1055.32, $0.35\times0.35\times0.30$ mm^3, triclinic, space group $P\bar{1}$, *a* = 9.932(2), *b* = 12.692(3), *c* = 13.290(3) Å, *α* = 114.46(3)°, *β* = 97.92(3)°, *γ* = 101.27(3)°, *V* = 1450.0(5) Å^3, *Z* = 1, $d_{calcd.}$ = 1.209 Mg m^{-3}, Mo-K_α radiation (graphite-monochromated, λ = 0.71073 Å), *T* = 100 K, θ_{range} 1.74 to 29.98°. Reflections measd. 15620, indep. 8385, R_{int} = 0.0391. Final *R* indices [$I>2\sigma(I)$]: R_1 = 0.0542, wR_2 = 0.1465.

(Br$_4$-4)(Br$_3$)$_2$Br$_2$: 0.014 mL (0.28 mmoL) Br_2 were added to a solution of 0.040 g (0.07 mmol) of **4** in 5 mL CH_3CN. The solution turned to a deep-brown colour. In one day the needle-shaped crystals of (Br$_4$-**4**)(Br$_3$)$_2$(Br)$_2$ were obtained from this solution at room temp; yield 0.083 g (0.055 mmoL, 78.0%). $C_{30}H_{40}Br_{12}N_{12}$ (1527.74): calcd. C 23.58, H 2.64, N 11.00; found C 23.80, H 3.00, N 11.04. ^{1}H NMR (399.89 MHz, CD_3CN): δ = 2.88 (s, 14 H, CH_3), 3.01 (s, 14 H, CH_3), 3.82 (s, 8 H, CH_2), 3.91 (s, 8 H, CH_2) ppm. Due to the low solubility of the salt, ^{13}C NMR spectra were not recorded. MS [ESI (%)]: *m*/*z* (%) = 444.1 (100) [Br$_4$-**4**]$^{2+}$, 887.9 (17) [Br$_4$-**4**]$^+$, 968.4 (10) [(Br$_4$-**4**)Br]$^+$. UV/Vis (CH_3CN, $c = 4.58\times10^{-5}$ mol L^{-1}): λ_{max} (ε in dm^{3}mol^{-1}cm^{-1}) = 269 (9.37×10^4), 218 (5.47×10^4) nm. IR (CsI): $\tilde{\nu}$ = 3012 (w), 2939 (w), 2878 (w), 2813 (w), 1664 (vs), 1619 (vs), 1462 (w), 1413 (w), 1367 (m), 1298 (s), 1233 (w), 1168 (w), 1039 (s), 981 (w), 893 (w), 790 (w), 756 (w), 680 (w), 645 (w), 574 (w), 500 (w) cm^{-1}. Crystal data for $C_{30}H_{40}Br_{12}N_{12}$: *M*r = 1527.66, $0.30\times0.20\times0.20$ mm^3, orthorhombic, space group *Pna*2(1), *a* = 14.688(3), *b* = 11.819(2), *c* = 27.188(5) Å, *V* = 4719.8(16) Å^3, *Z* = 4, $d_{calcd.}$ = 2.150 Mg m^{-3}, Mo-K_α radiation (graphite-monochromated, λ = 0.71073 Å), *T* = 100 K, θ_{range} 2.67 to 27.53°. Reflections measd. 33576, indep. 9988, R_{int} = 0.0563. Final *R* indices [$I>2\sigma(I)$]: R_1 = 0.0779, wR_2 = 0.1975.

[dimerH$_2$]I$_6$: 0.053 g (0.21 mmol) I_2 in 5 mL CH_3CN were added to a solution of 0.060 g (0.11 mmol) of **4** in 5 mL CH_3CN. The solution immediately turned to a deep-green colour. In one week yellow crystals were obtained from this solution at room temp. ^{1}H NMR

(399.89 MHz, CD_3CN): δ = 2.28–2.37 (d, 16 H, CH_2), 2.91–2.80 (d, 24 H, CH_3), 3.08–3.21 (d, 16 H, CH_2), 3.63–3.78 (d, 24 H, CH_3), 5.39 (s, 2 H), 7.29–7.32 (d, 4 H), 9.82 (s, 2 H) ppm. MS ESI (%): *m/z* (%) = 286.7 (11) $[dimer]^{4+}$, 571.4 (36) $[dimer]^{2+}$. Crystal data for $C_{60}H_{88}I_6N_{24}{\cdot}4.5H_2O$: *M*r = 1988.02, $0.13 \times 0.09 \times 0.09$ mm^3, triclinic, space group $P\bar{1}$, *a* = 13.367(7), *b* = 13.631(7), *c* = 22.734(12) Å, *α* = 101.24(1)°, *β* = 105.97(1)°, *γ* = 98.25(1)°, *V* = 3820(3) Å^3, *Z* = 2, d_{calc} = 1.729 Mg m^{-3}, Mo-K_α radiation (graphite-monochromated, λ = 0.71073 Å), *T* = 100 K, θ_{range} 2.0 to 26.5°. Reflections measd. 71146, indep. 15698, R_{int} = 0.0823. Final *R* indices [$I > 2\sigma(I)$]: R_1 = 0.0536, wR_2 = 0.1164.

[4(CoCl$_2$)$_2$]: 0.0273 g (0.21 mmoL) of $CoCl_2$ were added to a suspension of 0.060 g (0.11 mmoL) **4** in 20 mL CH_3CN. The solution immediately turned to a green colour. The mixture was stirred under reflux for 4 h. Afterwards the solution was concentrated to 10 mL. The green precipitate of [**4**($CoCl_2$)$_2$] was filtered off and washed three times with Et_2O; yield 0.0597 g (0.072 mmoL, 68.3%). Dark green crystals of the compound were obtained by layering CH_3CN solutions with ether at –18 °C. MS [ESI (%)]: *m/z* (%) = 287.2 (100) $[\mathbf{4}H_2]^{2+}$, 573.4 (40) $[\mathbf{4}H]^+$. UV/Vis (CH_3CN, *c* = 8.20×10^{-5} mol L^{-1}): λ_{max} (ε in dm^3 mol^{-1} cm^{-1}) = 247 (4.63×10^4), 407 (2.00×10^4), 570 (sh), 611, 686 nm. IR (CsI): $\tilde{\nu}$ = 2943 (w), 2886 (w), 1565 (vs), 1481 (m), 1413 (m), 1382 (s), 1290 (s), 1245 (m), 1157 (m), 1084 (w), 1046 (m), 985 (w), 916 (m), 885 (m), 806 (m), 647 (w), 584 (w), 466 (w) cm^{-1}. Crystal data for $C_{36}H_{53}Cl_4Co_2N_{15}$: *M*r = 955.59, $0.11 \times 0.09 \times 0.08$ mm^3, monoclinic, space group *C*2/*c*, *a* = 14.914(8), *b* = 20.012(9), *c* = 14.512(7) Å, *β* = 91.26(2)°, *V* = 4330(4) Å^3, *Z* = 4, $d_{calcd.}$ = 1.466 Mg m^{-3}, Mo-K_α radiation (graphite-monochromated, λ = 0.71073 Å), *T* = 100 K, θ_{range} 2.0 to 25.0°. Reflections measd. 35188, indep. 3829, R_{int} = 0.0531. Final *R* indices [$I > 2\sigma(I)$]: R_1 = 0.0708, wR_2 = 0.1612.

[3(NiCl$_2$)$_2$]: 118.1 mg (0.20 mmol) of **3** were dissolved in 15 mL abs. CH_2Cl_2 and cooled to –78 °C. The [(dme)$NiCl_2$] complex (89.3 mg, 0.41 mmol) was suspended in 15 mL abs. CH_2Cl_2 and also cooled to –78 °C. At this temperature, the solution of ttmgn was added slowly to the [(dme)$NiCl_2$] suspension. The reaction mixture was warmed up to room temp. over 18 h. The precipitate was filtered off and the solvent removed in vacuo from the filtrate. Subsequently, the crude product was washed with toluene (3×10 mL) to obtain a black solid in 88% yield (147.8 mg, 0.18 mmol). $C_{30}H_{52}Cl_4N_{12}Ni_2$ (840.01): calcd. C 42.89, H 6.24, N 20.01; found C 44.20, H 6.92, N 19.97. IR (CsI): $\tilde{\nu}$ = 3009 (w), 2931 (m), 2886 (m), 2793 (w), 1551 (vs), 1465 (s), 1404 (s), 1381 (s), 1319 (w), 1288 (w), 1157 (m), 1042 (m), 887 (w), 802 (w) cm^{-1}. MS (FAB^+): *m/z* (%) = 840.2 (12) $[M]^+$, 803.2 (18) $[M - Cl]^+$, 768.2 (5) $[M - 2Cl]^+$, 711.3 (100) $[M + H - NiCl_2]^+$. MS (HR-FAB^+): *m/z* (%) = 838.1840 (10.39) $[M]^+$, 803.2133 (18.02) $[M - Cl]^+$, 768.2383 (4.93) $[M - 2Cl]^+$. Exact masses for $[M]^+$: $[C_{30}H_{52}N_{12}{}^{35}Cl_4{}^{60}Ni_2]^+$ (13.1%): calcd. 840.1808; found 840.1806 (diff.: –0.2 mmu); $[C_{30}H_{52}N_{12}{}^{35}Cl_4{}^{58}Ni^{60}Ni]^+$ (10.4%): calcd. 838.1854; found 838.1840 (diff.: –1.4 mmu); $[C_{30}H_{52}N_{12}{}^{35}Cl_4{}^{58}Ni_2]^+$ (5.8%): calcd. 836.1899; found 836.1825 (diff.: –6.5 mmu); $[C_{30}H_{52}N_{12}{}^{35}Cl_3{}^{58}Ni^{60}Ni]^+$ (18.0%): calcd. 803.2165; found 803.2133 (diff.: +3.2 mmu). UV/Vis (CH_2Cl_2): λ (ε in dm^3 mol^{-1} cm^{-1}) = 250 (39397), 295 (9165), 387 (20592), 405 (18574), 466 (8265) nm.

[3(NiBr$_2$)$_2$]: 0.20 mmol **3** (118.1 mg) and 0.40 mmol [(dme)$NiBr_2$] (123.4 mg) each were dissolved in 15 mL abs. CH_2Cl_2 and cooled to –78 °C. The solution of ttmgn was added slowly to the [(dme)-$NiBr_2$] suspension at this temperature and the reaction mixture was warmed up to room temp. for 18 h. The precipitate was filtered off and the solvent removed in vacuo to obtain a black solid which was washed three times with 10 mL portions of toluene to obtain 118.3 mg of pure product (58%, 0.12 mmol). $C_{30}H_{52}Br_4N_{12}Ni_2$ (1017.82): calcd. C 35.40, H 5.15, N 16.51; found C 36.92, H 5.69, N 16.37. IR (CsI): $\tilde{\nu}$ = 3009 (w), 2932 (m), 2886 (m), 2792 (w), 1551 (vs), 1520 (vs), 1466 (s), 1404 (s), 1381 (s), 1319 (m), 1288 (m), 1234 (m), 1157 (m), 1041 (w), 887 (w), 709 (w) cm^{-1}. MS (FAB^+): *m/z* (%) = 1017.8 (16) $[M]^+$, 936.9 (22) $[M - Br]^+$, 799.1 (85) $[M - NiBr_2]^+$, 719.2 (55) $[M - Br - NiBr_2]^+$, 581.4 (55) $[\mathbf{3}H]^+$. MS (HR-FAB^+): *m/z* (%) = 1017.9841 ($[M]^+$, 100.00%), 937.0603 ($[M - Br]^+$, 99.10%). Exact masses for $[M]^+$: $[C_{30}H_{52}N_{12}{}^{81}Br_4{}^{58}Ni^{60}Ni]^+$ (23.0%): calcd. 1021.9751; found 1021.9807 (diff.: +5.6 mmu); $[C_{30}H_{52}N_{12}{}^{81}Br_4{}^{58}Ni_2]^+$ (57.0%): calcd. 1019.9797; found 1019.9828 (diff.: +3.1 mmu); $[C_{30}H_{52}N_{12}{}^{79}Br^{81}Br_3{}^{58}Ni_2]^+$ (100.0%): calcd. 1017.9817; found 1017.9841 (diff.: +2.4 mmu); $[C_{30}H_{52}N_{12}{}^{79}Br_2{}^{81}Br_2{}^{58}Ni_2]^+$ (85.4%): calcd. 1015.9837; found 1015.9846 (diff.: +0.9 mmu); $[C_{30}H_{52}N_{12}{}^{79}Br_3{}^{81}Br^{58}Ni_2]^+$ (41.0%): calcd. 1013.9858; found 1013.9861 (diff.: +0.3 mmu); $[C_{30}H_{52}N_{12}{}^{79}Br_4{}^{58}Ni_2]^+$ (9.1%): calcd. 1011.9878; found 1011.9922 (diff.: +4.4 mmu). UV/Vis (CH_2Cl_2): λ (ε in dm^3 mol^{-1} cm^{-1}) = 243 (41087), 303 (14728), 398 (18673), 407 (16663), 476 (5143) nm.

[3(Ni(acac)$_2$)$_2$]: 102.8 mg (0.40 mmol) Ni(acac)$_2$ as well as the **3** (118.1 mg, 0.20 mmol) were each dissolved in 15 mL abs. CH_2Cl_2 and cooled to –78 °C. The solution of **3** was then slowly added to the nickel-salt and the reaction mixture was warmed-up to room temp. for 18 h. The solvent was removed and the precipitate was filtered-off. The crude product was washed two times with 5 mL portions of abs. *n*-hexane to obtain 159.7 mg [**3**(Ni(acac)$_2$)$_2$] (73%, 0.15 mmol). $C_{50}H_{80}N_{12}O_8Ni_2$ (1094.63): calcd. C: 54.86, H 7.37, N 15.35; found C 55.52, H 7.39, N 13.25. IR (CsI): $\tilde{\nu}$ = 2993 (w), 2924 (w), 2888 (w), 2801 (w), 1605 (vs), 1558 (s), 1520 (s), 1466 (s), 1404 (s), 1257 (w), 1142 (m), 1018 (m), 918 (w), 748 (w) cm^{-1}. MS (FAB^+): *m/z* (%) = 992.7 (15) $[M - acac - H]^+$, 737.3 (60) $[M - Ni(acac)_2 - acac]^+$, 581.4 (100) $[\mathbf{3}]^+$. MS (HR-FAB^+): *m/z* (%) = 992.8489 (73.36) $[M - acac - H]^+$, 895.8131 (100) $[M - 2acac + H]^+$. MS (LIFDI, FD^+, CH_2Cl_2): *m/z* (%) = 580.17 (100) $[\mathbf{3}]^+$. UV/Vis (CH_2Cl_2): λ (ε in dm^3 mol^{-1} cm^{-1}) = 251 (56494), 300 (42842), 390 (17141), 415 (18237) nm.

[3(CuBr)$_2$]: To a solution of **3** (0.0600 g, 0.10 mmol) dissolved in 10 mL CH_3CN at 70 °C was added CuBr (0.0296 g, 0.20 mmol). The deep coloured reaction mixture was stirred for 15 min under reflux. Subsequently, the solution was slowly brought to room temp. After 24 h green, plate-like crystals of [**3**$(CuI)_2$] precipitated from this solution; yield 51.1% (0.0442 g, 0.05 mmol). $C_{30}H_{52}Br_2Cu_2N_{12}$ (864.16): calcd. C 41.53, H 6.04, N 19.36; found C 41.73, H 6.08, N 19.40. ^{1}H NMR (399.89 MHz, CD_2Cl_2): δ = 2.75 (s, 48 H, CH_3), 6.04 (s, 4 H) ppm. ^{13}C NMR (100.56 MHz, CD_2Cl_2): δ = 163.12, 141.33, 124.47, 117.08 (CH), 39.87 (CH_3) . UV/Vis (CH_3CN, *c* = 8.58×10^{-5} mol L^{-1}): λ_{max} (ε in dm^3 mol^{-1} cm^{-1}) = 419 (4.38×10^4) nm ppm. IR (CsI): $\tilde{\nu}$ = 3006 (w), 2965 (w), 2940 (w), 2872 (w), 2791 (w), 1525 (vs), 1462 (m), 1407 (s), 1370 (s), 1314 (w), 1266 (s), 1154 (m), 1017 (vs), 1154 (vs), 883 (s), 794 (vs), 705 (s), 627 (w), 561 (w) cm^{-1}. MS [ESI, *m/z* (%)]: 611.4 (30) $\{[\mathbf{3} - NC(NMe_2)_2]CuBr\}^+$. Crystal data for $C_{30}H_{52}Br_2Cu_2N_{12}$: *M*r = 867.74, $0.35 \times 0.30 \times 0.30$ mm^3, monoclinic, space group $P2_1/n$, *a* = 12.262(3), *b* = 10.725(2), *c* = 14.677(3) Å, *β* = 108.46(3)°, *V* = 1830.9(7) Å^3, *Z* = 1, d_{calc} = 1.574 Mg m^{-3}, Mo-K_α radiation (graphite-monochromated, λ = 0.71073 Å), *T* = 100 K, θ_{range} 1.89 to 31.04°. Reflections measd. 11663, indep. 5859, R_{int} = 0.0419. Final *R* indices [$I > 2\sigma(I)$]: R_1 = 0.0365, wR_2 = 0.0858.

[3(CuI)$_2$]: To a solution of **3** (0.0600 g, 0.10 mmoL) dissolved in 10 mL CH_3CN at 70 °C was added CuI (0.0394 g, 0.20 mmol). The dark reaction mixture was stirred for 15 min under reflux. Subsequently, the solution was slowly brought to room temp. After 24 h green plate-like crystals of [**3**(CuI)$_2$] precipitated from this solution; yield 54.7% (0.0544 g, 0.06 mmol). $C_{30}H_{52}Cu_2I_2N_{12}$ (965.76): calcd. C 37.32, H 5.84, N 17.40; found C 37.96, H 5.40, N 17.32. ^{1}H NMR (399.89 MHz, CD_2Cl_2): δ = 2.77 (s, 48 H, CH_3), 6.03 (s, 4 H) ppm. ^{13}C NMR (100.56 MHz, CD_2Cl_2): δ = 163.81, 141.29, 124.43, 117.00 (CH), 40.17 (CH_3) ppm. UV/Vis (CH_3CN, $c = 8.05\times10^{-5}$ mol L^{-1}): λ_{max} (ε in dm^{3}mol^{-1}cm^{-1}) = 420 (5.18×10^4) nm. IR (CsI): $\tilde{\nu}$ = 3006 (w), 2932 (m), 2872 (m), 2802 (w), 1529 (vs), 1459 (m), 1396 (s), 1373 (s), 1318 (vs), 1318 (w), 1280 (w), 1236 (w), 1154 (vs), 1032 (m), 943 (w), 887 (w), 843 (w), 772 (w), 702 (w), 627 (w), 546 (w) cm^{-1}. MS [ESI, *m*/*z* (%)]: 626.1 (100) {[**3** – NC(NMe$_2$)$_2$ – 2CH$_3$]CuI}$^+$, 899.2 (40) {[**3** – 4CH$_3$ – 3H]Cu$_2$I$_2$}$^+$. Crystal data for $C_{30}H_{52}Cu_2I_2N_{12}$: *M*r = 961.72, $0.40\times0.35\times0.35$ mm^3, monoclinic, space group $P2_1/n$, a = 12.359(3), b = 10.728(2), c = 15.239(3) Å, β = 108.10(3)°, V = 1920.5(7) Å^3, Z = 2, d_{calc} = 1.663 Mg m^{-3}, Mo-K_α radiation (graphite-monochromated, λ = 0.71073 Å), T = 100 K, θ_{range} 1.86 to 30.09°. Reflections measd. 10999, indep. 5605, R_{int} = 0.0171. Final R indices [$I > 2\sigma(I)$]: R_1 = 0.0226, wR_2 = 0.05.

[3(CuBr$_4$)$_2$]: 0.01 mL (0.206 mmoL) Br_2 in 5 mL CH_3CN were added to a suspension of 0.0890 g (0.103 mmol) of [**3**(CuBr)$_2$] in 10 mL CH_3CN. The solution turned to a deep-brown colour. Subsequently the solvent was removed until 5 mL were left and the solution was filtered off. The product of the reaction was obtained as a black powder which was washed with diethyl ether and dried in vacuo; yield 0.112 g (0.083 mmol, 81%). $C_{30}H_{52}Br_8Cu_2N_{12}$ (1347.24): calcd. C 26.74, H 3.90, N 12.48; found C 22.97, H 3.41, N 10.67. ^{1}H NMR (399.89 MHz, CD_3CN): δ = 3.26 (s, 48 H, CH_3), 7.44 (s, 4 H) ppm. UV/Vis: (CH_3CN, $c = 4.88\times10^{-7}$ mol L^{-1}): λ_{max} (ε in dm^{3}mol^{-1}cm^{-1}) = 374 (1.89×10^4), 683 (0.90×10^4), 746 (1.29×10^4) nm. IR (CsI): $\tilde{\nu}$ = 2973 (w), 2923 (w), 2793 (w), 1637 (vs), 1596 (vs), 1525 (vs), 1466 (vs), 1410 (vs), 1366 (m), 1269 (s), 1225 (m), 1173 (s), 1151 (s), 1106 (w), 1062 (s), 1043 (s), 935 (w), 891 (s), 831 (s), 787 (s), 687 (m), 650 (w), 620 (w), 553 (w) cm^{-1}. MS [ESI, *m*/*z* (%)]: 290.2 (34) [**3**]$^{2+}$, 436.4 (9) [**3**-NC(NMe$_2$)$_2$-2CH$_3$]$^+$, 803.2 (100) {(**3**)CuBr$_2$}$^+$, 947.1 (32) {(**3**)Cu$_2$Br$_3$}$^+$. Crystal data for $C_{30}H_{52}Br_8Cu_2N_{12}$: *M*r = 1347.20, $0.16\times0.13\times0.11$ mm^3, orthorhombic, space group $Pmc2_1$, a = 28.717(3), b = 8.5347(8), c = 21.435(2) Å, V = 5253.4(8) Å^3, Z = 4, d_{calc} = 1.703 Mg m^{-3}, Mo-K_α radiation (graphite-monochromated, λ = 0.71073 Å), T = 100 K, θ_{range} 1.9 to 28.3°. Reflections measd. 40538, indep. 12846, R_{int} = 0.0518. Final R indices [$I > 2\sigma(I)$]: R_1 = 0.0448, wR_2 = 0.1041.

X-ray Crystallographic Study: Suitable crystals were taken directly out of the mother liquor, immersed in perfluorinated polyether oil, and fixed on top of a glass capillary. Measurements were made on Nonius-Kappa or Bruker AXS Smart 1000 CCD diffractometers with low-temperature unit using graphite-monochromated Mo-K_α radiation. The temperature was set to 100 K. The data collected were processed using the standard Nonius or Bruker AXS software.[29,30] All calculations were performed using the SHELXTPLUS software package. The structures were solved either by direct methods with the SHELXS-97 program and refined with the SHELXL-97 program[31,32] or by the charge-flip procedure[33,34] and refined by full-matrix least-squares methods based on F^2 against all unique reflections. All non-hydrogen atoms were given anisotropic displacement parameters. Hydrogen atoms were generally input at calculated positions and refined with a riding model.[35] The crystals of [**4**(CoCl$_2$)$_2$] and [**3**(CuBr$_4$)$_2$] were found to contain strongly disordered solvent of crystallization. Electron density attributed to the disordered solvent molecules was removed from the structures (and the corresponding F_{obs}) with the BYPASS procedure, as implemented in PLATON (SQUEEZE).[36] Graphical handling of the structural data during solution and refinement was performed with XPMA.[37] Pseudo-merohedral twinning was detected in the crystal of [**3**(CuBr$_4$)$_2$] (refined fractions 0.57 and 0.43). The crystals of [dimerH$_2$]I$_6$·4.5H$_2$O were non-merohedrally twinned; refinement was against de-twinned data from the major (ca. 80%) component (all relevant observations including singles that also occurred in composites).[36] The hydrogen atoms resulting from N protonation were found in difference Fourier Syntheses and refined riding on the corresponding nitrogen atoms (cf. Scheme 3).

CCDC-800633 [for (**4**H$_2$)Cl$_2$], -770435 [for **1**(TCNQ)$_2$], -800632 [for (Br$_4$-**4**)(Br$_3$)$_2$Br$_2$], -800634 [for (dimerH$_2$)I$_6$], -800629 [for **4**-(CoCl$_2$)$_2$], -800631 [for **3**(CuBr)$_2$], -800630 [for **3**(CuI)$_2$], -800628 [for **3**(CuBr$_4$)$_2$] contain the supplementary crystallographic data for this paper. These data can be obtained free of charge from The Cambridge Crystallographic Data Centre via www.ccdc.cam.ac.uk/data_request/cif.

Quantum Chemical Calculations: Quantum chemical calculations were carried out with the GAUSSIAN 03[38] or TURBOMOLE programs.[39,40] The B3LYP functional[41,42] was used in combination with the SVP[43] basis set for calculations on [**3**(NiCl$_2$)$_2$] and with a 6-311G** basis set for [Br$_4$-**4**]$^{4+}$.

Supporting Information (see also the footnote on the first page of this article): CV curves recorded for **4** dissolved in CH_3CN at different scan speeds, IR spectra recorded for **1**(TCNQ)$_2$ and TCNQ (KBr discs), UV/Vis spectrum of **1**(TCNQ)$_2$ in CH_2Cl_2 solution, Molecular structure of the product obtained from reaction between **4** and I_2, Structure of [**3**(NiCl$_2$)$_2$] from B3LYP/SVP calculations, Comparison between structural parameters (bond lengths in Å, bond angles in deg) obtained for (Br$_4$-**4**)[(Br$_3$)$_2$Br$_2$] with those calculated (B3LYP/ 6-311G**) for (Br$_4$-**4**)$^{4+}$ in the gas phase.

Supporting Information (see footnote on the first page of this article): CV curves recorded for **4** dissolved in CH_3CN at different scan speeds, IR spectra recorded for **1**(TCNQ)$_2$ and TCNQ (KBr discs), UV/Vis spectrum of **1**(TCNQ)$_2$ in CH_2Cl_2 solution, molecular structure of the product obtained from reaction between **4** and I_2, structure of [**3**(NiCl$_2$)$_2$] from B3LYP/SVP calculations, comparison between structural parameters (bond lengths in Å, bond angles in °) obtained for (Br$_4$-**4**)(Br$_3$)$_2$Br$_2$ with those calculated (B3LYP/6-311G**) for (Br$_4$-**4**)$^{4+}$ in the gas phase.

Acknowledgments

The authors gratefully acknowledge financial support by the Deutsche Forschungsgemeinschaft (DFG).

[1] *Superbases for Organic Synthesis* (Ed.: T. Ishikawa), John Wiley & Sons, John Wiley & Sons, Ltd., Chichester, U. K. **2009**.
[2] R. W. Alder, P. S. Bowman, W. R. S. Steele, D. R. Winterman, *J. Chem. Soc., Chem. Commun.* **1968**, 723–724.
[3] R. Schwesinger, *Nachr. Chem. Tech. Lab.* **1990**, *38*, 1214–1226; and references given therein .
[4] V. Raab, E. Gauchenova, A. Merkoulov, K. Harms, J. Sundermeyer, Z. B. Maksić, *J. Am. Chem. Soc.* **2005**, *127*, 15738–15743.
[5] There is an approved and clear definition of the term "superbase": P. Caubère, *Chem. Rev.* **1993**, *93*, 2317–2334; see also the first chapter in ref.[1]: "*The term 'superbase' should only be*

applied to bases resulting from a mixing of two (or more) bases leading to a new basic species possessing inherent new properties. The term "superbase" does not mean a base is thermodynamically and/or kinetically stronger than another, instead it means that a basic reagent is created by combining the characteristics of several different bases." The guanidine ttmgn combines the basicity of guanidino groups with Alder's concept of a proton sponge. Therefore ttmgn clearly qualifies as "superbase".

[6] For further recent contributions in the field of strong organic bases, see: a) I. Kaljurand, A. Kütt, L. Sooväli, T. Rodima, V. Mäemets, I. Leito, I. A. Koppel, *J. Org. Chem.* **2005**, *70*, 1019–1028; b) A. A. Kolomeitsev, I. A. Koppel, T. Rodima, J. Barten, E. Lork, G.-V. Röschenthaler, I. Kaljurand, A. Kütt, I. Koppel, V. Mäemets, I. Leito, *J. Am. Chem. Soc.* **2005**, *127*, 17656–17666.

[7] V. Raab, J. Kipke, R. M. Gschwind, J. Sundermeyer, *Chem. Eur. J.* **2002**, *8*, 1682–1693.

[8] B. Kovačević, Z. B. Maksić, *Chem. Eur. J.* **2002**, *8*, 1694–1702.

[9] D. Margetic, in: *Superbases for Organic Synthesis* (Ed.: T. Ishikawa), John Wiley & Sons, Ltd., Chichester, U. K., **2009**, chapter 2, p. 9–48, and references given therein.

[10] A. Peters, U. Wild, O. Hübner, E. Kaifer, H.-J. Himmel, *Chem. Eur. J.* **2008**, *14*, 7813–7821.

[11] A. Peters, E. Kaifer, H.-J. Himmel, *Eur. J. Org. Chem.* **2008**, 5907–5914.

[12] D. Emeljanenko, A. Peters, V. Vitske, E. Kaifer, H.-J. Himmel, *Eur. J. Inorg. Chem.* **2010**, 4783–4789.

[13] B. Kovaćević, Z. B. Maksić, *Org. Lett.* **2001**, *3*, 1523–1526.

[14] A. Peters, U. Wild, E. Kaifer, H.-J. Himmel, unpublished results.

[15] P. Roquette, A. Maronna, M. Reinmuth, M. Enders, H.-J. Himmel, *Inorg. Chem.* **2011**, in press.

[16] V. Vitske, C. König, E. Kaifer, O. Hübner, H.-J. Himmel, *Eur. J. Inorg. Chem.* **2010**, 115–126.

[17] a) P. J. Bailey, S. Pace, *Coord. Chem. Rev.* **2001**, *214*, 91–141; b) F. T. Edelmann, *Adv. Organomet. Chem.* **2008**, *57*, 183–352; and references cited therein; c) S. Herres-Pawlis, *Nachr. Chem.* **2009**, *57*, 20–23.

[18] P. Roquette, A. Maronna, A. Peters, E. Kaifer, H.-J. Himmel, Ch. Hauf, V. Herz, E.-W. Scheidt, W. Scherer, *Chem. Eur. J.* **2010**, *16*, 1336–1350.

[19] U. Wild, O. Hübner, A. Maronna, M. Enders, E. Kaifer, H. Wadepohl, H.-J. Himmel, *Eur. J. Inorg. Chem.* **2008**, 4440–4447.

[20] a) D. Domide, C. Neuhäuser, E. Kaifer, H. Wadepohl, H.-J. Himmel, *Eur. J. Inorg. Chem.* **2009**, 2170–2178; b) M. Reinmuth, U. Wild, E. Kaifer, M. Enders, H. Wadepohl, H.-J. Himmel, *Eur. J. Inorg. Chem.* **2009**, 4795–4808.

[21] T. Yamasaki, N. Ozaki, Y. Saika, K. Ohta, K. Goboh, F. Nakamura, M. Hashimoto, S. Okeya, *Chem. Lett.* **2004**, *33*, 928–929.

[22] C. Trumm, E. Kaifer, O. Hübner, H.-J. Himmel, *Eur. J. Inorg. Chem.* **2010**, 3102–3108.

[23] D. Emeljanenko, A. Peters, N. Wagner, J. Beck, E. Kaifer, H.-J. Himmel, *Eur. J. Inorg. Chem.* **2010**, 1839–1846.

[24] a) A. Peters, C. Trumm, M. Reinmuth, D. Emeljanenko, E. Kaifer, H.-J. Himmel, *Eur. J. Inorg. Chem.* **2009**, 3791–3800; b) P. Roquette, C. König, O. Hübner, E. Kaifer, M. Enders, H.-J. Himmel, *Eur. J. Inorg. Chem.* **2010**, 4770–4782.

[25] A. Rembaum, A. M. Hermann, F. E. Stewart, F. Gutmann, *J. Phys. Chem.* **1969**, *73*, 513–520.

[26] I. Zanon, C. Pecile, *J. Phys. Chem.* **1983**, *87*, 3657–3664.

[27] G. Bellucci, R. Bianchini, R. Ambrosetti, *J. Chem. Soc. Perkin Trans. 2* **1987**, 39–45.

[28] http://ewww.mpi-muelheim.mpg.de/bac/logins/bill/julX_en.php.

[29] DENZO-SMN, Data processing software, Nonius, **1998**; http://www.nonius.com.

[30] G. M. Sheldrick, *TWINABS*, Bruker AXS, **2008**.

[31] a) G. M. Sheldrick, *SHELXS-97*, *Program for Crystal Structure Solution*, University of Göttingen, Germany, **1997**; http://shelx.uni-ac.gwdg.de/SHELX/index.html.

[32] *International Tables for X-ray Crystallography*, vol. 4, Kynoch Press, Birmingham, UK, **1974**.

[33] a) G. Oszlányi, A. Sütö, *Acta Crystallogr., Sect. A* **2004**, *60*, 134; b) G. Oszlányi, A. Sütö, *Acta Crystallogr., Sect. A* **2005**, *61*, 147–152.

[34] a) L. Palatinus, *SUPERFLIP*, EPF Lausanne, Switzerland, **2007**; b) L. Palatinus, G. Chapuis, *J. Appl. Crystallogr.* **2007**, *40*, 786–790.

[35] G. M. Sheldrick, *SHELXL-97*, *Program for Crystal Structure Refinement*, University of Göttingen, Germany, **1997**; http://shelx.uni-ac.gwdg.de/SHELX/index.html.

[36] a) P. v. d. Sluis, A. L. Spek, *Acta Crystallogr., Sect. A* **1990**, *46*, 194–201; b) A. L. Spek, *PLATON*, Utrecht University, The Netherlands; A. L. Spek, *J. Appl. Crystallogr.* **2003**, *36*, 7–13.

[37] L. Zsolnai, G. Huttner, *XPMA*, University of Heidelberg, **1994**; http://www.uni-heidelberg.de/institute/fak12/AC/huttner/software/software.html.

[38] M. J. Frisch, G. W. Trucks, H. B. Schlegel, G. E. Scuseria, M. A. Robb, J. R. Cheeseman, V. G. Zakrzewski, J. A. Montgomery Jr., R. E. Stratmann, J. C. Burant, S. Dapprich, J. M. Millam, A. D. Daniels, K. N. Kudin, M. C. Strain, O. Farkas, J. Tomasi, V. Barone, M. Cossi, R. Cammi, B. Mennucci, C. Pomelli, C. Adamo, S. Clifford, J. Ochterski, G. A. Petersson, P. Y. Ayala, Q. Cui, K. Morokuma, D. K. Malick, A. D. Rabuck, K. Raghavachari, J. B. Foresman, J. Cioslowski, J. V. Ortiz, B. B. Stefanov, G. Liu, A. Liashenko, P. Piskorz, I. Komaromi, R. Gomperts, R. L. Martin, D. J. Fox, T. Keith, M. A. Al-Laham, C. Y. Peng, A. Nanayakkara, C. Gonzalez, M. Challacombe, P. M. W. Gill, B. Johnson, W. Chen, M. W. Wong, J. L. Andres, C. Gonzalez, M. Head-Gordon, E. S. Replogle, J. A. Pople, *Gaussian 03*, Gaussian Inc., Pittsburgh, PA, **1998**.

[39] R. Ahlrichs, M. Bär, M. Häser, H. Horn, C. Kölmel, *Chem. Phys. Lett.* **1989**, *162*, 165–169.

[40] O. Treutler, R. Ahlrichs, *J. Chem. Phys.* **1995**, *102*, 346–354.

[41] P. J. Stephens, F. J. Devlin, C. F. Chabalowski, M. J. Frisch, *J. Phys. Chem.* **1994**, *98*, 11623–11627.

[42] C. Lee, W. Yang, R. G. Parr, *Phys. Rev. B* **1988**, *37*, 785–789.

[43] F. Weigend, R. Ahlrichs, *Phys. Chem. Chem. Phys.* **2005**, *7*, 3297–3305.

Received: November 15, 2010
Published Online: February 18, 2011

